SU-8-based microneedles for *in vitro* neural applications

2010 J. Micromech. Microeng. 20 064014

(http://iopscience.iop.org/0960-1317/20/6/064014)

J. Micromech. Microeng. **20** (2010) 064014 (6pp) doi:10.1088/0960-1317/20/6/064014

SU-8-based microneedles for *in vitro* neural applications

Ane Altuna[1], Gemma Gabriel[2,3], Liset Menéndez de la Prida[4], María Tijero[1], Anton Guimerá[2,3], Javier Berganzo[1], Rafa Salido[1], Rosa Villa[2] and Luis J Fernández[1]

[1] MEMS/MST Department, Ikerlan S. Coop., 20500 Mondragón, Spain
[2] Instituto de Microelectrónica de Barcelona (IMB-CNM), CSIC, Campus UAB, 08913 Bellaterra, Barcelona, Spain
[3] Centro de Investigación Biomédica en Red, Biomateriales y Nanomedicina (CIBER-BBN), Zaragoza, Spain
[4] Instituto Cajal, CSIC, 28002 Madrid, Spain

E-mail: ane.altuna@ikerlan.es

Received 27 November 2009, in final form 23 March 2010
Published 1 June 2010
Online at stacks.iop.org/JMM/20/064014

Abstract
This paper presents novel design, fabrication, packaging and the first *in vitro* neural activity recordings of SU-8-based microneedles. The polymer SU-8 was chosen because it provides excellent features for the fabrication of flexible and thin probes. A microprobe was designed in order to allow a clean insertion and to minimize the damage caused to neural tissue during *in vitro* applications. In addition, a tetrode is patterned at the tip of the needle to obtain fine-scale measurements of small neuronal populations within a radius of 100 μm. Impedance characterization of the electrodes has been carried out to demonstrate their viability for neural recording. Finally, probes are inserted into 400 μm thick hippocampal slices, and simultaneous action potentials with peak-to-peak amplitudes of 200–250 μV are detected.

1. Introduction

Neuroscience is a constantly growing field and new biomedical tools are required for further advances. Multisite electrode microneedles are interesting biomedical tools because they provide optimum communication between the macroscopic world and neurons. Such an interaction is based on fine-scale measurements of neural activity.

In recent years different materials have been studied for the fabrication of these probes, silicon being the most popular one. However, the main drawbacks of this material are its rigidity and brittleness. It has been demonstrated that tissue is damaged due to the rigidity of the silicon during experimental applications [1, 2], and also, a high risk of breaking exists during the manipulation of silicon-based probes. Recent studies suggest that polymers could be an alternative to silicon [1–5]. Polyimide and BCB (benzocyclobutene) have already been used for the fabrication of neural devices [6, 7]. The problems related to the brittleness of traditional silicon probes can be avoided using polyimide or BCB devices. However, both of them are so excessively flexible that deformation of the tip occurs when they penetrate the tissue, and therefore other materials are included to make the device more robust [4, 7]. In this work, microneedles made exclusively of SU-8 (SU-8 50, MicroChem Corp., Newton, MA) are introduced. The fabrication of this device is a low-cost process and at the same time the device is reusable. SU-8-based probes can be used many more times, whereas silicon tends to break. The elastic modulus of this polymer is in the same order as the BCB and polyimide but the SU-8 allows the fabrication of devices within a wider thickness range [7, 8]. Therefore, microneedle rigidity can be controlled by adjusting its thickness. Apart from this feature, the SU-8 polymer has been chosen because of its high-aspect-ratio capability [9]. Vertical sidewall profiles can be patterned on devices with a length in the order of centimeters while still being narrow ($<$100 μm). The use of photolithography enables a good dimensional control over the entire thickness, and thus, a needle-shaped device is obtained. Furthermore, a suitable degree of biocompatibility of SU-8 has already been reported although a deeper study is still required for further application [10]. Recently, some authors published the first reports of a biocompatible SU-8-based probe used for *in vitro* neural tests. The results obtained from cultures of different types of cells strongly support that specifically

processed SU-8-based devices could be well suited for neural interface applications [11].

In our previous work, the functional viability of thick SU-8-based microneedles was studied [12]. They were tested in rat neural tissue and successful results were obtained for *ex vivo* and *in vivo* applications. The thickness of these needles is in the order of 200 μm, which is required to integrate a microchannel. However, the design of these probes is not appropriate for fine-scale neural applications. When inserted into brain slices, these needles drag the tissue due to their large dimension. Also, the electrodes are too large to measure the electrical activity from small neuronal ensembles. In this work a novel design, fabrication procedure and packaging of SU-8 microneedles for neural recording are proposed. Reduced electrode dimensions are required in order to better monitorize neural activity. In addition, narrower and thinner needles are necessary in order to ensure a good insertion into a thin neural tissue slice. All these design requirements entail new fabrication challenges, mainly alternative releasing methods and electrode patterning processes. Moreover, an alternative procedure is proposed for future fabrication to improve electrode patterning and achieve better electrode–tissue contact. The packaging of the device is also adapted to the experimental procedure in order to facilitate recordings. Impedance spectroscopy shows the typical capacitive behavior of electrodes, and *in vitro* tests demonstrate the probe viability as a tool for recording neural activity.

2. Design and fabrication

A schematic overview of the microneedle design is presented in figure 1(*a*). As it can be observed, three different sections are distinguished: insertion area, microneedle body and connection head.

2.1. Insertion area

The insertion area is 180 μm long since the tip needs to be inserted into the tissue to a depth of about 100–150 μm. In order to ensure a good penetration, a sharp tip is designed as shown in figure 1(*b*). In addition, the insertion area is 30 μm thick to minimize the damage induced to the tissue during the experimental application. In order to measure the activity from small neuronal groups, which is the main objective of this application, the electrode diameter is set at 20 μm, quite comparable to neuron size. The electrode configuration is a tetrode (see figure 1(*b*)); thus, 80 μm wide probes have been designed in order to fit the electrodes at the tip.

2.2. Microneedle body

The width of this area increases gradually from 80 μm to 1 mm along its length, the thickness being kept at 100 μm to make the needle mechanically stronger. In order to test different needle sizes in the experimental applications, 2 and 3 cm body lengths have been designed.

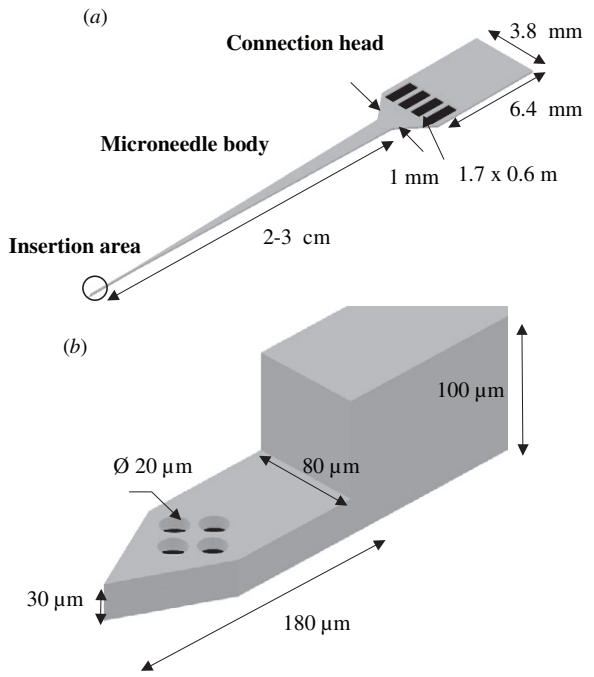

Figure 1. (*a*) Schematic drawing of the microneedle and (*b*) schematic drawing of the tip.

2.3. Connection head

This section is 6.4 mm long, 3.8 mm wide and 100 μm thick to make the needle easy to handle and package. This is the place where the external contact pads are located. There are four 1.7 mm long and 0.6 mm wide contact pads. These dimensions are fixed to guarantee an easy connection of the needle to the printed circuit board (PCB).

2.4. Basic fabrication procedure

The fabrication of the microneedle starts with an aluminum deposition on a silicon wafer by sputtering, as shown in figure 2(*I*). This is a sacrificial layer that allows the release of the needles from the substrate at the end of the fabrication process. A 10 μm thick SU-8 layer is spun and soft baked, heating up to 65 °C for 2 min and up to 95 °C for 7 min, figure 2(*II*). Then, an UV dose of 140 mJ cm^{-2} is applied by standard photolithography, and finally a post bake for 2 min at 65 °C and 4 min at 95 °C is applied. Once this layer is developed, chromium (50 nm) and gold (100 nm) layers are deposited by sputtering, figure 2(*III*). In order to define the electrodes, a positive resin is patterned, figure 2(*IV*). This layer is used as a mask for gold and chromium patterning by wet chemical etching, figure 2(*V*). Then, the resin covering the electrodes is removed, figure 2(*VI*), and a 20 μm thick SU-8 passivation layer is deposited to cover the metallic tracks, figure 2(*VII*). Afterward, a 70 μm thick SU-8 layer is spun on top, figure 2(*VII*), heated up to 65 °C for 10 min and up to 95 °C for 30 min as a soft bake. Then, an UV dose of 140 mJ cm^{-2} is applied and a post bake of 2 min at 65 °C and 4 min at 95 °C is performed.

In our previous SU-8-based fabrication procedure of microneedles [12], the SU-8 layers were deposited on top

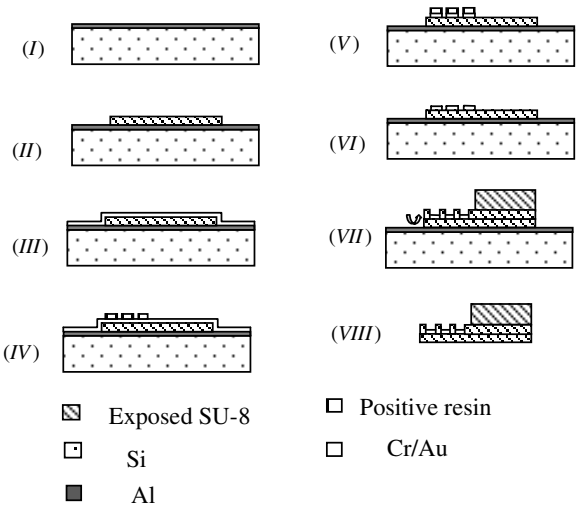

Figure 2. Neural probe basic fabrication sequence.

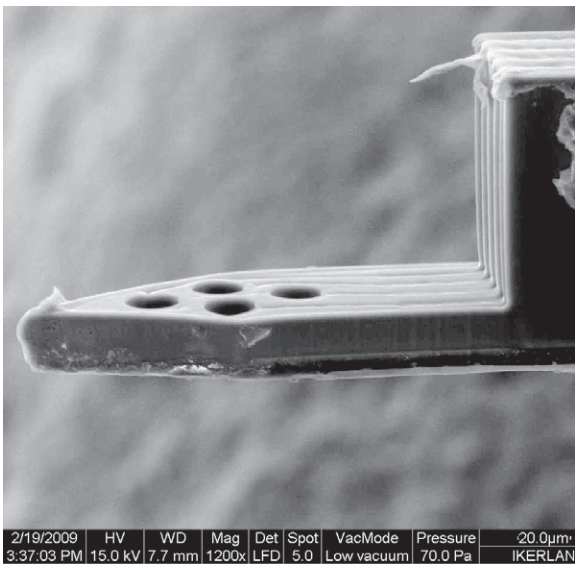

Figure 3. SEM picture of a microneedle tip.

of a Kapton™ film. The low adhesion between Kapton™ and SU-8 enabled a mechanical release of the probes once the fabrication was finished. In this case, the reduced dimensions of the probe make a mechanical-based release impossible. Alternatively, microneedles are released from the silicon wafer by introducing them in a phosphoric acid solution, figure 2(*VIII*). A scanning electron microscope (SEM) picture of a typical needle can be observed in figure 3.

In this fabrication process, a combination of different soft bake times and exposition doses has been tested in order to optimize the protocol for very long and narrow electrodes. The narrowest metallic tracks (3.5 μm) are defined by heating the resin up to 90 °C and applying high exposure doses.

2.5. Discussion and alternative fabrication procedure

In the basic fabrication procedure, although the electrodes seem to be patterned on a flat area, a slight increase of height at the edges of each microneedle is noticed after the 10 μm SU-8 layer is developed, figure 2(*II*). This makes it difficult to obtain a good patterning on the irregular area. The narrowest tracks, figure 2(*IV*), cannot be well defined during the UV exposure of the positive resin due to the irregularity mentioned above. Furthermore, there is also an edge bead in the wafer that can be appreciated once the SU-8 layer is spin coated. As a consequence of these two facts, the narrowest metallic tracks are not correctly defined in all the microneedles yielding about 60% successful probes. Therefore, an alternative fabrication method is designed (see the next paragraph) which is expected to improve the electrode patterning because the positive resin is now spun on a flat substrate, figure 4(*IV*), instead of on a 10 μm thick SU-8-developed layer.

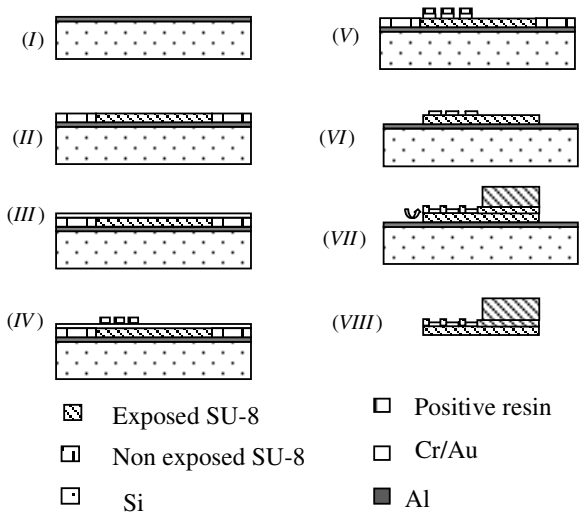

Figure 4. Neural probe alternative fabrication sequence.

In the alternative fabrication procedure, after the aluminum deposition, as shown in figure 4(*I*), a 20 μm thick SU-8 layer will be spun and heated up to 65 °C for 2 min and up to 95 °C for 7 min, figure 4(*II*). Afterward, an UV dose of 140 mJ cm^{-2} will be applied and a post bake will be performed by heating the layer up to 65 °C for 2 min and up to 95 °C for 4 min. Then, chromium (50 nm) and gold (100 nm) will be deposited by sputtering over the non-developed SU-8 layer, figure 4(*III*). After the metallization process the positive resin will be photopatterned, figure 4(*IV*), in order to perform gold and chromium wet chemical etchings, figure 4(*V*). In the next step, the structural 20 μm thick SU-8 layer will be developed with ultrasonic agitation and the positive resin that is covering the electrodes will be removed, figure 4(*VI*). Next, a 10 μm thick passivation layer and a 70 μm thick layer will be developed as in the previously described fabrication process, figure 4(*VII*). Finally, the microneedles will be released by aluminum wet etching, figure 4(*VIII*).

In both fabrication proposals, the insertion area thickness is 30 μm in order to minimize the damage induced to the tissue and ensure the insertion of the device into the tissue. In the first procedure, a 20 μm thick SU-8 layer is on a 10 μm thick SU-8 layer, and in the second one the layers would be inverted, as seen in figure 5. The future version may present an advantage over the actual one because the distance between the

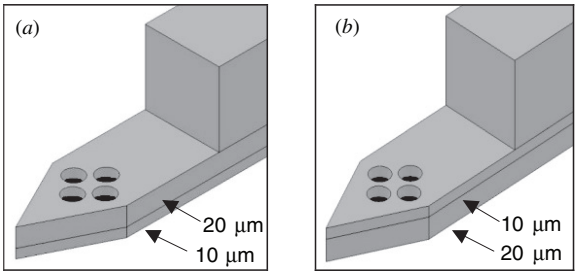

Figure 5. (*a*) Current configuration: 20 μm passivation layer and (*b*) future configuration: 10 μm passivation layer.

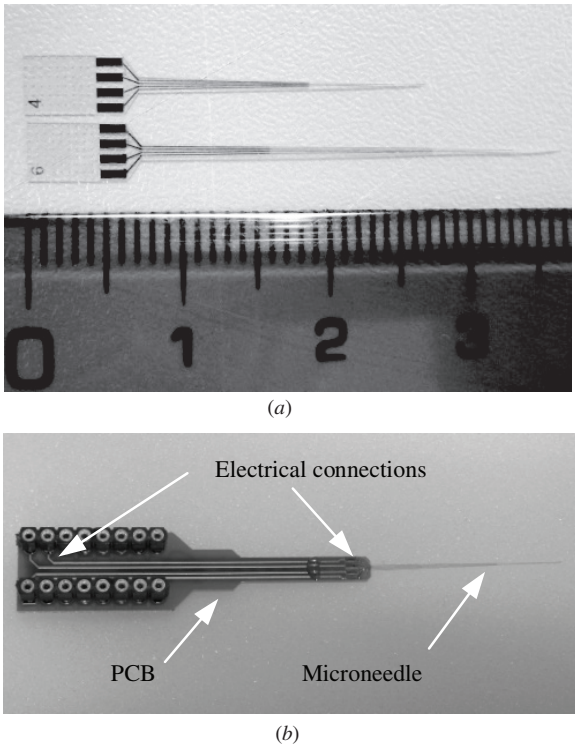

Figure 6. (*a*) Microneedles of different lengths, (*b*) packaged microneedle.

electrode and the surface would be 10 μm and the electrode–tissue contact could improve.

3. Packaging

The packaging allows easy handling of SU-8 probes and electrical data acquisition from tests. A conductive adhesive (Elecolit 3005 from Panacol-Eosol) is chosen to connect the microneedle pads to the PCB. After applying the conductive adhesive onto the microneedle and the PCB, the probe is aligned and pressed against the PCB [8]. Then, the probe and the PCB are heated up to 60 °C for half an hour until the adhesive is completely cured. Next, Loctite 3430 is deposited in the corners of the microprobe to fix the device mechanically onto the PCB. After 12 h, the microneedles are introduced in a saline solution to verify the electrical connections. In figure 6(*a*), two microneedles of different lengths can be observed right after the release step, and in figure 6(*b*), a packaged microneedle is shown.

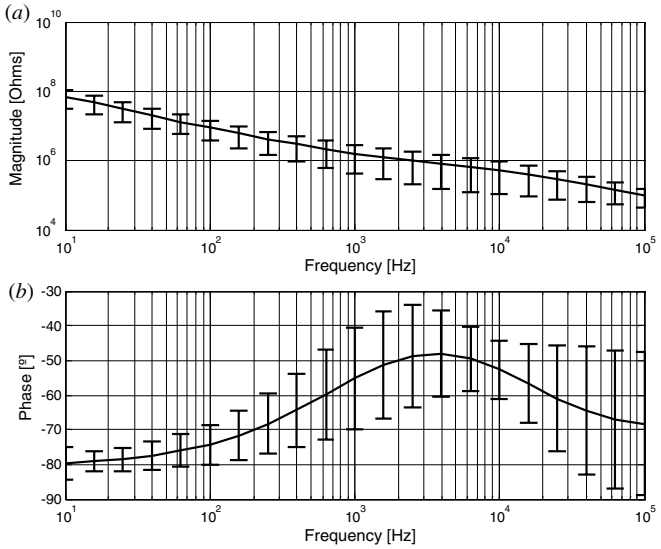

Figure 7. Impedance modulus (*a*) and phase shift (*b*) of gold electrodes. Average measurements from electrodes are shown. Error bars represent standard deviation ($n = 8$).

4. Characterization

4.1. Impedance spectroscopy

Impedance measurements were conducted in order to characterize the electrode–electrolyte interface. Two-wire electrochemical impedance spectroscopy measurements were performed with each of the four electrodes versus a platinum reference electrode. The electrical properties of the gold electrodes were estimated by measuring the impedance and phase shift versus frequency from 10 Hz to 10^5 Hz in a physiological saline solution (0.9 wt% NaCl with a nominal resistivity of 71.3 Ω cm). Gold was used as a recording site metal because of its excellent surface inertness and because it provides no native oxide. This metal minimizes the capacitive component at the electrode–electrolyte interface. In figure 7, impedance modulus results are summarized (average measurements and standard deviation from two probes, $n = 8$ electrodes). These show a great dependence on the frequency which corresponds to a typical capacitive behavior of the electrode double layer. Furthermore, the high impedance values registered are typical of small-sized electrodes. In the future, a coating will be applied on the electrode area (e.g. electrochemical platinization or carbon nanotube deposition [13, 14]) in order to improve the electrical recordings by decreasing the impedance values. At the same time, this process will decrease the dispersion recorded in the modulus and phase angle.

4.2. In vitro tests

Two probes were tested using hippocampal slices. Briefly, horizontal slices were prepared from normal adult rats and kept in interface conditions using standard bathing solutions [15]. Recordings were obtained from the CA3 region of the hippocampus and three slices were tested at 32 °C. The microneedle tip was gently inserted to a depth of about 150 μm

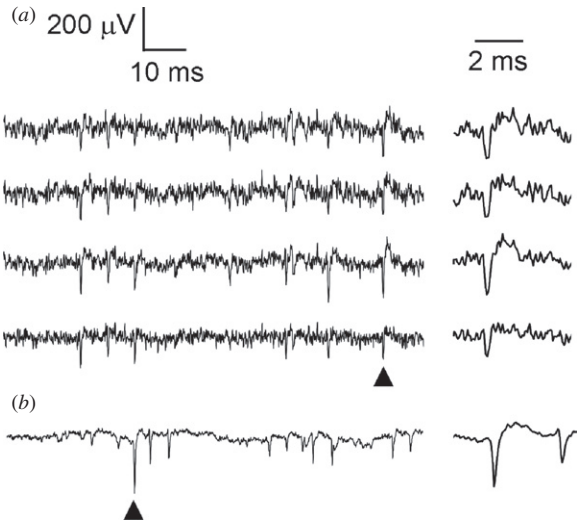

Figure 8. Extracellular spontaneous signals recorded *in vitro* using the SU-8-based microneedles (*a*) and a conventional low impedance electrode, ∼400 kΩ (*b*). Both recordings were obtained from the same slice. Action potentials from several neurons were distinguishable with both probes. The different noise level is attributable to difference in the electrode shape and impedance. Arrowheads point to one of such action potentials recorded in all four electrodes of the SU-8 probe, which is expanded on the right. Spike waveforms, duration and amplitude are all consistent with the signal emerging from a single neuron, as recorded with conventional electrodes.

into a 400 μm thick hippocampal slice and spontaneous signals were recorded in the band of 10 Hz to 10 kHz. As shown in figure 8, signals demonstrated the typical shape of extracellularly recorded action potentials superimposed on noise. The noise level was in the range of 22–30 μV rms (mean 27.3 μV rms, $n = 8$ electrodes from 2 probes), which mostly accounted for the thermal noise from the electrodes (10 μV rms) and the setup noise that is about 12 μV rms. Detectable action potentials had peak-to-peak amplitudes up to 200–250 μV, quite comparable to those recorded with conventional tetrodes [16]. However, large spikes (>300 μV rms) were not observed with these probes; probably, due to the poor electrode–neuron interface caused by the presence of a 20 μm passivation gap between the electrode and the tissue. This electrode–neuron interface could be improved by reducing the thickness of the passivation layer following the alternative fabrication method. In addition, filling the gap by electrochemical platinization or carbon nanotube deposition can also be useful. This would also result in lower impedances and improved signal to noise ratio.

5. Conclusions

This work demonstrates for the first time the viability of SU-8-based microneedles to measure fine-scale neural activity. These narrow and thin probes have been successfully processed in order to minimize tissue damage and slice dragging. Moreover, reduced electrodes are obtained to record the activity from small neuronal ensembles. All these improvements have been easily verified due to the packaging specially developed for this application. Probe functionality for neural recording has been demonstrated by *in vitro* testing. However, it is desirable to distinguish more and bigger action potentials over the noise in further tests. In the near future, the electrodes based on the alternative fabrication process will be closer to the tissue, and thus, spiking activity from closer neurons is expected to be optimally detected. On the other hand, several rough coatings will be tested to increase the effective area of the electrode and thus improve the signal to noise ratio.

Acknowledgments

This work was supported by the Basque Government under the Etortek-Microsystems programme and also funded by grants from the Spanish Ministry MICINN (BFU2009-07989), the ERANET-Neuron project EPINet from the EU Commission under FP7, MICINN (EUI2009-04093) and MEC (TEC2006-14186-CO2-01).

References

[1] Cheung K C and Renaud P 2006 BioMEMS for medicine: on-chip cell characterization and implantable microelectrodes *Solid State Electron.* **50** 551–7
[2] Subbaroyan J, Martin D C and Kipke D R 2005 A finite-element model for the mechanical effects of implantable microelectrodes in the cerebral cortex *J. Neural Eng.* **2** 103–13
[3] Ziegler D, Suzuki T and Takeuchi S 2006 Fabrication of flexible neural probes with built-in microfluidic channels by thermal bonding of parylene *J. Microelectromech. Syst.* **15** 1477–82
[4] Lee K K, He J, Singh A, Massia S, Ehteshami G, Kim B and Raupp G 2004 Polyimide-based intracortical neural implant with improved structural stiffness *J. Micromech. Microeng.* **14** 32–7
[5] O'Brien D P, Nichols T R and Allen M G 2001 Flexible microelectrode arrays with integrated insertion devices *Proc. IEEE MEMS Conf.* pp 216–9
[6] Metz S, Bertsch A, Bertrand D and Renaud P 2004 Flexible polyimide probes with microelectrodes and embedded microfluidic channels for simultaneous drug delivery and multi-channel monitoring of bioelectric activity *Biosens. Bioelectron.* **19** 1309–18
[7] Lee K, Massia S and He J 2005 Biocompatible benzocyclobutene-based intracortical neural implant with surface modification *J. Micromech. Microeng.* **15** 2149–55
[8] Tijero M, Gabriel G, Cairo J, Altuna A, Hernández R, Villa R, Berganzo J, Blanco F J, Salido R and Férnandez L J 2009 SU-8 microprobe with microelectrodes for monitoring electrical impedance in living tissues *Biosens. Bioelectron.* **24** 2410–6
[9] Despont M, Lorenz H, Fahrni N, Brugger J, Renaud P and Vettiger P 1997 High-aspect-ratio, ultrathick, negative-tone near-UV photoresist for MEMS applications *Proc. 10th IEEE Ann. Workshop on Micro Electro Mechanical Systems (Nagoya, Japan, 26–30 January, 1997)* pp 518–22
[10] Voskerician G, Shive M S, Shawgo R B, von Recum H, Anderson J M, Cima M J and Langer R 2003 Biocompatibility and biofounding of MEMS drug delivery devices *Biomaterials* **24** 1959–67
[11] Cho S-H, Lu H M, Cauller L, Romero-Ortega M I, Lee J-B and Hughes G A 2008 Biocompatible SU-8-based

microprobes for recording neural spike signals from regenerated peripheral nerve fibers *IEEE Sensors J.* **11** 1830–6

[12] Fernández L J, Altuna A, Tijero M, Gabriel G, Villa R, Rodríguez M J, Batlle M, Vilares R, Berganzo J and Blanco F J 2009 Study of functional viability of SU-8 based microneedles for neural applications *J. Micromech. Microeng.* **19** 025007

[13] Gabriel G, Gómez R, Bongard M, Benito N, Fernández E and Villa R 2009 Easily made single-walled carbon nanotube surface microelectrodes for neuronal applications *Biosens. Bioelectron.* **24** 1942–8

[14] Gabriel G, Erill I, Caro J, Gómez R, Riera D, Villa R and Godignon P 2007 Manufacturing and full characterization of silicon carbide-based multi-sensor micro-probes for biomedical applications *Microelectron. J.* **38** 406–15

[15] Menendez de la Prida L, Huberfeld G, Cohen I and Miles R. 2006 Threshold behavior in the initiation of hippocampal population bursts *Neuron* **49** 131–42

[16] Csicsvari J, Henze D A, Jamieson B, Harris K D, Sirota A, Barthó P, Wise K D and Buzsáki G 2003 Massively parallel recording of unit and local field potentials with silicon-based electrodes *J. Neurophysiol* **90** 1314–23